

UNCLASSIFIED

AD NUMBER

ADB026151

LIMITATION CHANGES

TO:

Approved for public release; distribution is unlimited.

FROM:

Distribution authorized to U.S. Gov't. agencies only; Test and Evaluation; MAR 1978. Other requests shall be referred to Rome Air Development Center, Attn: OCSE, Griffiss AFB, NY 13441.

AUTHORITY

RADC, USAF ltr, 17 May 1978

THIS PAGE IS UNCLASSIFIED

THIS REPORT HAS BEEN DELIMITED
AND CLEARED FOR PUBLIC RELEASE
UNDER DOD DIRECTIVE 5200.20 AND
NO RESTRICTIONS ARE IMPOSED UPON
ITS USE AND DISCLOSURE.

DISTRIBUTION STATEMENT A

APPROVED FOR PUBLIC RELEASE;
DISTRIBUTION UNLIMITED.

RADC-TR-78-25
Interim Report
March 1978

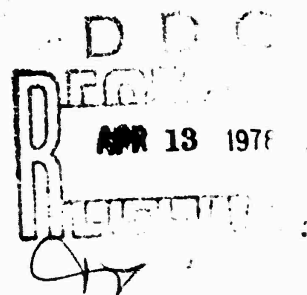


LINEAR SPACE-VARIANT IMAGE RESTORATION OF PHOTON-
LIMITED IMAGES

Stanford University

Sponsored by
Defense Advanced Research Projects Agency (DoD)
ARPA Order No. 2646

Distribution limited to U.S. Government agencies only;
test and evaluation; March 1978. Other requests for
this document must be referred to RADC (OCSE), Griffiss
AFB NY 13441.



The views and conclusions contained in this document are those of
the authors and should not be interpreted as necessarily representing
the official policies, either expressed or implied, of the Defense
Advanced Research Projects Agency or the U. S. Government.

ROME AIR DEVELOPMENT CENTER
Air Force Systems Command
Griffiss Air Force Base, New York 13441

DDC FILE COPY

AD B026151

APPROVED:

[illegible]

Do not return this copy. Retain or destroy.

LINEAR SPACE-VARIANT IMAGE RESTORATION OF PHOTON-LIMITED IMAGES

J. F. Belsher
J. W. Goodman

Contractor: Stanford University
Contract Number: F30602-75-C-0228
Effective Date of Contract: 1 April 1975
Contract Expiration Date: 28 February 1978
Short Title of Work: Fundamental Limits to the
Performance of a Compensated
Imaging System
Program Code Number: 8E20
Period of Work Covered: Jan 77 - Oct 77

Principal Investigator: Dr. J. W. Goodman
Phone: 415 497-3304

Project Engineer: Donald W. Hanson
Phone: 315 330-3144
Autovon 587-3144

Distribution limited to U.S. Government agencies only; test and evaluation; March 1978. Other requests for this document must be referred to RADC (OCSE), Griffiss AFB NY 13441.

This research was supported by the Defense Advanced Research Projects Agency of the Department of Defense and was monitored by Donald W. Hanson (OCSE), Griffiss AFB NY 13441 under Contract F30602-75-C-0228.

D D C
APR 13 1978

UNCLASSIFIED

SECURITY CLASSIFICATION OF THIS PAGE (When Data Entered)

18 REPORT DOCUMENTATION PAGE		READ INSTRUCTIONS BEFORE COMPLETING FORM	
1. REPORT NUMBER RADC-TR-78-25	2. GOVT ACCESSION NO.	3. RECIPIENT'S CATALOG NUMBER	
4. TITLE (and Subtitle) LINEAR SPACE-VARIANT IMAGE RESTORATION OF PHOTON-LIMITED IMAGES		5. TYPE OF REPORT & PERIOD COVERED Interim Report 1 Jan - 1 Oct 77	
7. AUTHOR(s) J. F. Belsher J. W. Goodman		6. PERFORMING ORG. REPORT NUMBER N/A	
8. PERFORMING ORGANIZATION NAME AND ADDRESS Stanford University Stanford CA 94305		9. CONTRACT OR GRANT NUMBER(s) F30602-75-C-0228, ARPA Order-2646	
11. CONTROLLING OFFICE NAME AND ADDRESS Defense Advanced Research Projects Agency 1400 Wilson Blvd Arlington VA 22209		10. PROGRAM ELEMENT, PROJECT, TASK AREA & UNIT NUMBERS 62301E 26460405	
14. MONITORING AGENCY NAME & ADDRESS (if different from Controlling Office) Rome Air Development Center (OCSE) Griffiss AFB NY 13441		12. REPORT DATE March 78	
		13. NUMBER OF PAGES 28	
		15. SECURITY CLASS. (of this report) UNCLASSIFIED	
16. DISTRIBUTION STATEMENT (of this Report) Distribution limited to U.S. Government agencies only; test and evaluation; March 1978. Other requests for this document must be referred to RADC (OCSE), Griffiss AFB NY 13441.		15a. DECLASSIFICATION/DOWNGRADING SCHEDULE N/A	
17. DISTRIBUTION STATEMENT (of the abstract entered in Block 20, if different from Report) Same			
18. SUPPLEMENTARY NOTES RADC Project Engineer: Donald W. Hanson (OCSE)			
19. KEY WORDS (Continue on reverse side if necessary, and identify by block number) Image processing Space-variant filtering Image quality measurement Adaptive optics			
20. ABSTRACT (Continue on reverse side if necessary, and identify by block number) Results of analyses to determine image quality versus number of photons in the image are given. Conditions which lead to the least-mean-square-error filter being space-variant are given. Formulation of the linear space-variant filter for discrete signals is given.			

DD FORM 1 JAN 73 1473 EDITION OF 1 NOV 65 IS OBSOLETE

UNCLASSIFIED

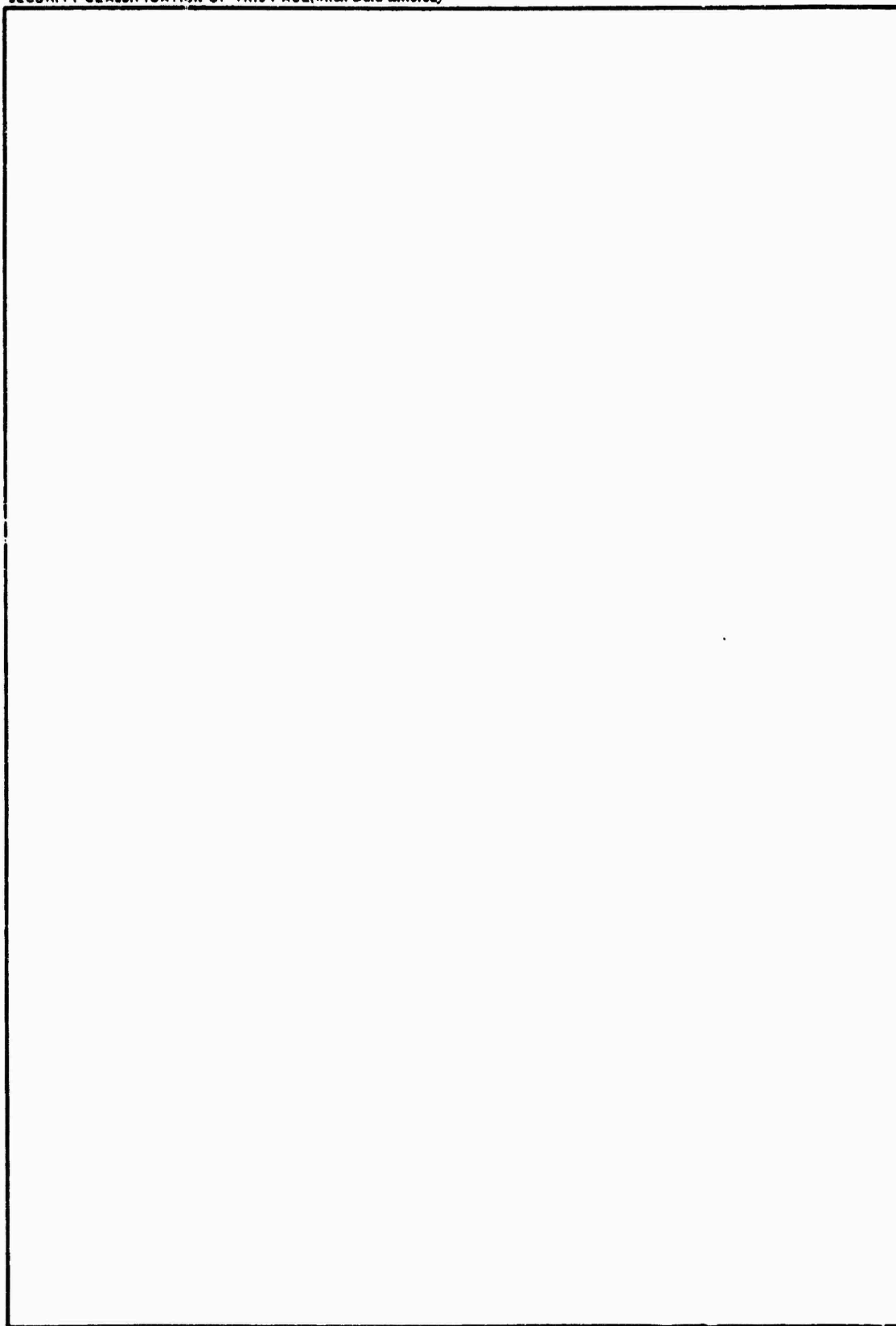
SECURITY CLASSIFICATION OF THIS PAGE (When Data Entered)

332550

284

UNCLASSIFIED

SECURITY CLASSIFICATION OF THIS PAGE(When Data Entered)



UNCLASSIFIED

SECURITY CLASSIFICATION OF THIS PAGE(When Data Entered)

I. INTRODUCTION

Research in the time period covered by this report has been concentrated primarily on the subject of linear, space-variant restoration of blurred, photon limited images. However, some effort has also been devoted to extending our previous work on photon limitations in compensated imaging, particularly an extension of the results presented in RADC report #RADC-TR-77-165.

In section II we discuss the extensions mentioned above. Section III briefly describes some unsuccessful attempts at formulating the space-variant filtering problem in continuous notation. Section IV deals with a more successful discrete formulation of this problem. Finally, section V outlines the numerical computations now being undertaken.

II. FURTHER PERFORMANCE PREDICTIONS FOR A PRE- AND POST-COMPENSATED IMAGING SYSTEM

In two previous technical reports (RADC-TR-76-382 and RADC-TR-77-165) the photon-limited performance of a specific compensated imaging system was analyzed. The primary results of this analysis were two figures showing restored bandwidth $\Delta\tilde{\omega}$ and quality factor Q as a function of the total number \bar{N} of photoevents intercepted by the system for a variety of combinations of pre- and post-processing. Figure 8 of RADC-TR-76-382 showed that the restored bandwidth of the pre- and post-compensated system reached the diffraction-limited bandwidth when approximately 10^7 photoevents were intercepted by the system, this conclusion being valid for a point-source object.

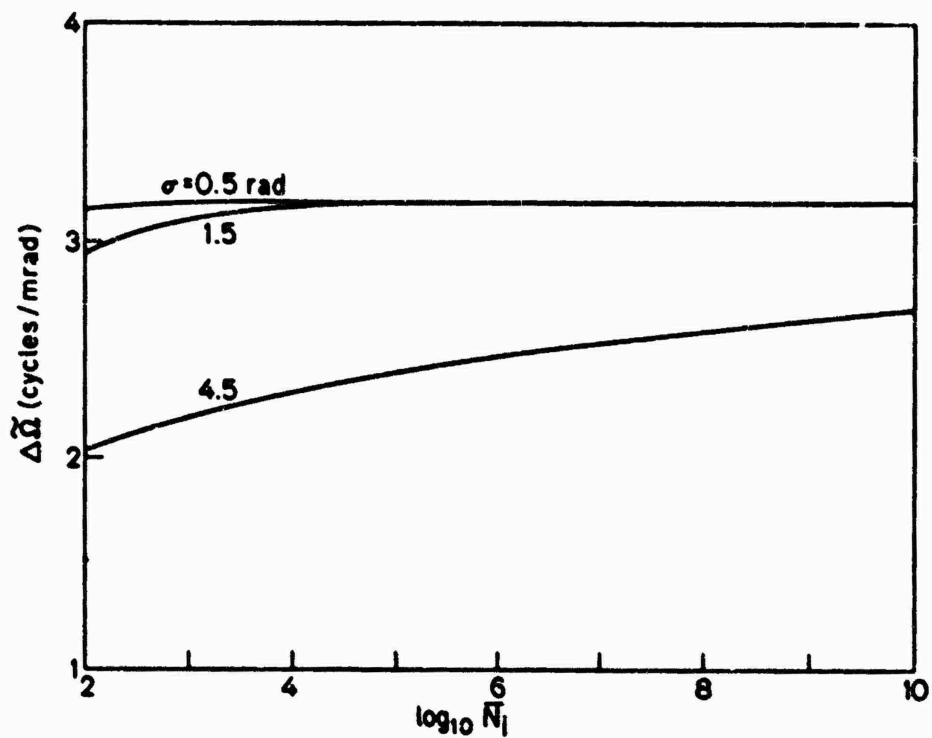
In the derivation of these curves, certain assumptions about the system were made. These included assumptions that the atmospheric

coherence diameter r_0 was 10cm, that the system employed a shearing interferometer with 317 subapertures, and that the ratio of image integration time to wavefront sensor integration time was 10^4 . In addition it was assumed that the system employed a fixed splitting ratio such that 90% of the incoming light was sent to the wavefront sensor and 10% was sent to the image detector. The 90% splitting ratio was found to be nearly optimum, although the maximum is very broad.

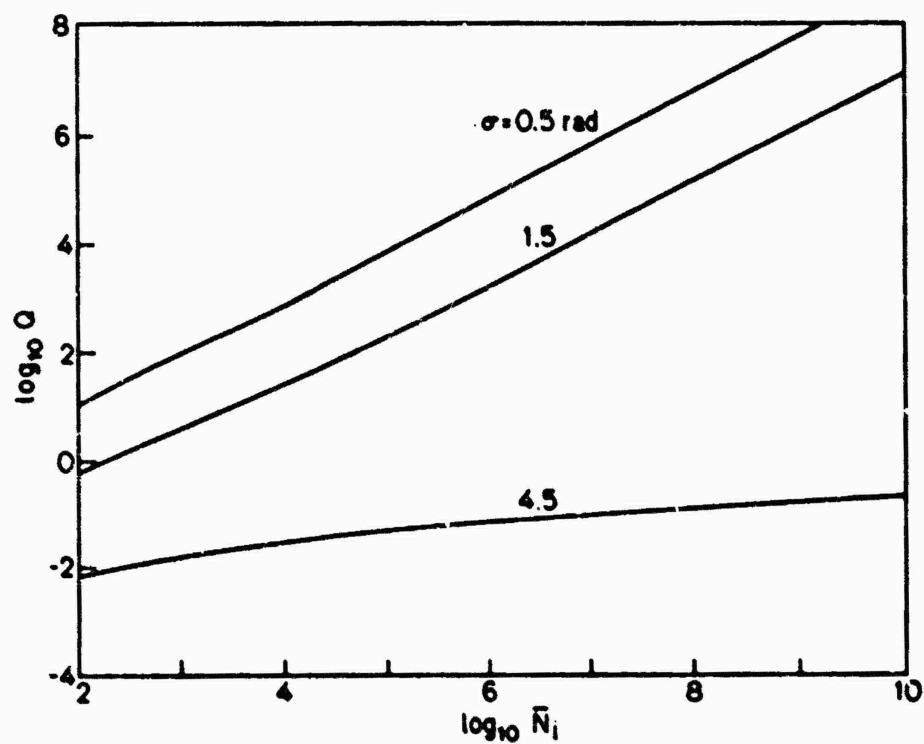
Concerns were expressed by members of the Review Group that the number of photoevents required in the image ($10\% \times 10^7 = 10^6$ photoevents) might saturate the detector. Examination of the calculations showed that the requirement for 10^7 total photoevents was dominated by the flux required for satisfactory operation of the wavefront sensor, and it was speculated that the use of smaller splitting ratios (less than 10% to the image) would reduce the dynamic range required of the detector without seriously degrading the quality of the final restored image.

The correctness of this speculation was investigated by setting the performance of the wavefront sensor at certain fixed levels, and calculating restored bandwidth and image quality as a function of the total number of photoevents in the detected image. This latter quantity is represented by the symbol \bar{N}_i .

The results of these calculations are presented in Fig. 1. Part (a) shows the restored bandwidth $\Delta\tilde{\omega}$ (cycles/m rad) vs. \bar{N}_i , while part (b) shows the quality factor Q vs. \bar{N}_i . In both cases, three curves are presented, one for each of three levels of performance of the wavefront sensor. The parameter α represents the residual rms wavefront error (measurement noise plus fitting error) and takes on the values 0.5 radians, 1.5 radians and 4.5 radians. These numbers correspond to 0.08, 0.24 and 0.72 waves of rms error.



(a)



(b)

Figure 1: Restored bandwidth (a) and quality factor (b) vs. average number of image photoevents for fixed levels of performance of the wavefront sensor.

As can be seen from part (a) of the figure, when $\sigma = 0.5$ radians, the restored bandwidth is essentially indistinguishable from the diffraction limited bandwidth, even for as few as 100 photoevents in the image. For $\sigma = 1.5$ radians, about 10^4 image photoevents are needed to achieve the diffraction-limited restored bandwidth. Finally, when $\sigma = 4.5$ radians, the performance of the wavefront sensor is so poor that enormous numbers of image photoevents (considerably more than 10^{10}) are needed to achieve diffraction-limited performance.

Hopefully, this set of calculations will provide some indication of the numbers of image photoevents that will be required to achieve satisfactory quality in the final restored images.

III. CONTINUOUS FORMULATION OF THE SPACE-VARIANT RESTORATION PROBLEM

All previous analysis of the performance of pre- and post-compensated imaging systems has assumed that the final post-detection restoration filter is a linear space-invariant Wiener filter. This type of filtering is known to be optimum only when the signal and noise are uncorrelated stationary random processes and when the noise statistics are gaussian. In the regime of photon-limited imaging, the noise is non-gaussian and signal-dependent, and it is therefore reasonable to assume that some form of linear, space-variant filtering or nonlinear filtering will perform better than the simple filtering used in earlier analyses.

The change from linear space-invariant filtering to more complex filtering strategies has associated with it a cost in computational complexity and processing time. It is natural therefore to inquire as to how much image quality is gained by these more complex methods, and at what price.

In this report we consider only linear, space-variant, least-mean-square filtering. Such filters depend on certain average properties of the class of images anticipated, but do not depend on the particular image detected on any given trial. Techniques which perform a filtering operation that depends on the particular image detected are generally non-linear, and will be considered in later work under this contract.

Figure 2 illustrates the nature of the least-square-filtering problem of interest to us here. For simplicity a one-dimensional space variable x is used throughout. The object radiance distribution $o(x)$ is assumed to be a random process. In general the statistics $o(x)$ may be non-stationary; hence its autocorrelation function $R_o(x_1, x_2)$ is a function of the two space coordinates x_1 and x_2 rather than just their difference.

The object radiance distribution is subjected to a linear blur, described by an impulse response or point-spread function that is in general space-variant, and is represented by $b(x_1, x_2)$. The result is a classical image irradiance $i(x)$ incident on the detector, where

$$i(x) = \int_{-\infty}^{\infty} b(x, \xi) o(\xi) d\xi \quad (1)$$

Through the detection process, a detected image $d(x)$ is generated. As implied by the semi-classical theory of photodetection, $d(x)$ is a doubly stochastic Poisson impulse process, with space-variant mean $\lambda(x)$ related to the classical image intensity through

$$\lambda(x) = \frac{\eta T}{h\nu} i(x) \quad (2)$$

where η is the quantum efficiency, T the integration time, h is Planck's constant, and $\bar{\nu}$ is the mean optical frequency. The detected

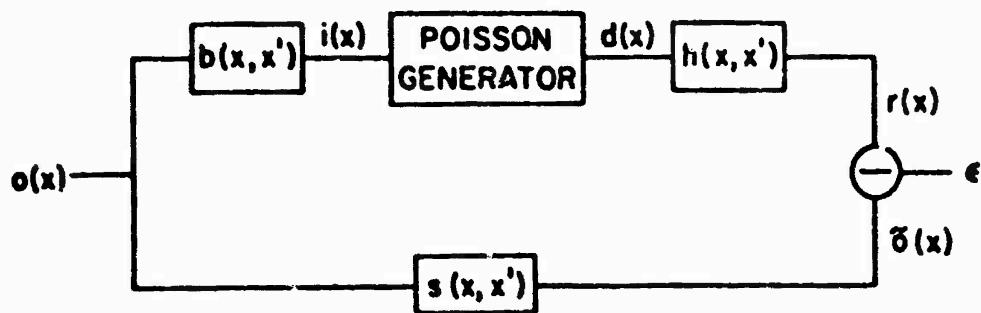


Figure 2: Least square filtering problem in diagrammatic form.

image $d(x)$ is passed through a linear, space-variant restoration filter with impulse response $h(x_1, x_2)$, yielding a restored image $r(x)$ given by

$$r(x) = \int_{-\infty}^{\infty} h(x, n) d(n) dn \quad (3)$$

The impulse response $h(x_1, x_2)$ is chosen to minimize the mean-square difference between the restored image $r(x)$ and an ideally filtered object $\tilde{d}(x)$. In general, the ideal filter may be space-variant with impulse response $s(x_1, x_2)$.

At this point it is natural to inquire as to what set of conditions can lead to a least-mean-square filter which is space-variant rather than space-invariant. To answer this question, we must first present some theoretical results which can be derived without much difficulty, and which are presented here without proof. The impulse response $h(x, x'')$ of the restoration filter which achieves least mean-square error is the solution of the integral equation.

$$\begin{aligned} \int_{-\infty}^{\infty} h(x, x'') R_d(x', x'') dx'' \\ = \int_{-\infty}^{\infty} s(x, x'') R_{d_0}(x', x'') dx'' \end{aligned} \quad (4)$$

Here $s(x, x'')$ is again the known impulse response of the ideal filter, while R_d and R_{d_0} are also known functions, given by

$$\begin{aligned} R_d(x', x'') &= E[d(x') d(x'')] \\ &= \frac{\eta I}{h\nu} \bar{I}(x') \delta(x' - x'') + \frac{\eta^2 I^2}{h^2 \nu^2} R_i(x', x'') \end{aligned} \quad (5)$$

$$\begin{aligned}
 R_{do}(x', x'') &= E[d(x')o(x'')] \\
 &= \frac{\eta \bar{T}}{h\nu} R_{io}(x', x'')
 \end{aligned} \tag{6}$$

where $\bar{T}(x')$ is the mean value of the image irradiance at x' , averaged over the ensemble of possible objects, $R_i(x', x'')$ is the autocorrelation function of the image irradiance, and $R_{io}(x', x'')$ is the cross-correlation function of the image irradiance and the object radiance. More specifically,

$$\bar{T}(x') = \int_{-\infty}^{\infty} b(x', x'') \bar{o}(x'') dx'' \quad . \tag{7}$$

$$\begin{aligned}
 R_i(x', x'') &= E[i(x')i(x'')] = \iint_{-\infty}^{\infty} b(x', \xi) b(x'', \eta) \\
 &\quad \cdot R_o(\xi, \eta) d\xi d\eta \quad ,
 \end{aligned} \tag{8}$$

$$R_{io}(x', x'') = E[i(x')o(x'')] = \int_{-\infty}^{\infty} b(x', \xi) R_o(\xi, x'') d\xi \quad , \tag{9}$$

where $\bar{o}(x'')$ is the mean object radiance at x'' ; and $R_o(\xi, \eta)$ is the autocorrelation function of the object radiance distribution.

Examination of this somewhat bewildering array of results leads one to the conclusion that the least-mean-square-error filter will be space-variant if any one of the following conditions hold:

- (1) The mean value $\bar{o}(x)$ of the object radiance distribution is not constant (i.e., is indeed a function of x), the expectation being over the entire ensemble of possible objects;
- (2) The autocorrelation function $R_o(\xi, \eta)$ of the object is non-stationary (i.e., depends on both ξ and η , rather than just their difference).

- (3) The impulse response $b(x_1, x_2)$ of the blur is space variant (i.e., non isoplanatic);
- (4) The impulse response $s(x_1, x_2)$ of the ideal filter is space variant.

We now examine each of these conditions in the context of the compensated imaging problem. Consider first the mean value $\bar{o}(x)$ of the object radiance distribution over the object ensemble. All space-objects are of course spatially bounded (i.e., of finite extent), and for this reason we could argue that $\bar{o}(x)$ is always a function of x . However, in any real measurement we look in on the object process with a finite measurement window, and it is possible that over this measurement window the expected object radiance is constant. On the other hand, it is not difficult to identify situations in which the mean object radiance would be a function of position within the measurement window. An example would be when the object of interest is far smaller than the measurement window, but due to tracking errors its position within the window obeys some non-uniform probability density function. In such a case $\bar{o}(x)$ is definitely a function of x , and therefore the least-mean-square restoration filter must of necessity be space-variant.

Turning to condition (2), we would also expect the object autocorrelation function $R_o(\xi, \eta)$ to be non-stationary under the conditions described above. Alternatively, even if there are no tracking errors, and the object has constant mean radiance in the field of interest, we might expect the central portion of the object (i.e., the main body) to have different textural appearance than the extremities (appendages consisting of arms, booms, etc.), and hence a non-stationary autocorrelation function

might be required to properly describe the second-order statistics of the object. Again a space-variant restoration filter would be required for optimum performance.

As for condition (3), space variance of the blur is anticipated when the size of the object exceeds the size of the isoplanatic region of the compensated imaging system. Under such conditions, space-variant restoration is again required if the smallest possible mean-square error is to be achieved.

Finally, condition (4), space-variance of the ideal filter, can generally be ignored. In most cases of interest it is appropriate to use as an ideal filter the diffraction limited telescope itself. Such a filter is space invariant, and as a consequence it is always safe in these problems to assume that the impulse response s depends only on the difference of its two variables.

At this point, we have introduced arguments that demonstrate that in most practical applications of compensated imaging, the ideal post-detection restoration filter will be space variant. It is quite another matter to say precisely what the optimum filter is, and to calculate its performance. The chief difficulties involved in this task are:

- (1) Specification of reasonable models for $\bar{o}(x)$, $R_o(x, x')$ and $b(x, x')$; and
- (2) Solution of the integral equation (4) for these models.

Several attempts at finding a solution for various specific cases have not met with success. Cases examined included an object which is a "windowed" stationary process (and therefore nonstationary), and an object with a nonstationary autocorrelation function of the form

$$R_0(x_1, x_2) = \Gamma\left(\frac{x_1 + x_2}{2}\right) \delta(x_1 - x_2) \quad (10)$$

Since even these idealistically chosen cases proved unsolvable, it was decided that the continuous approach would have to be abandoned in favor of a discrete approach. For a discrete formulation of the problem, the necessity of solving an integral equation to find the required impulse response h is replaced by the necessity of solving a matrix equation. The latter is far easier to do, in general. We therefore turn to a discussion of the discrete approach to the problem at hand.

IV. DISCRETE FORMULATION OF THE SPACE-VARIANT RESTORATION PROBLEM

In this section we treat the same problem addressed in section III, but using a discrete representation of the various physical quantities involved. We begin with a discussion of the discrete representation itself and the physical meaning of the quantities involved.

(a) Discrete Notation

The continuous object radiance distribution $o(x)$ is replaced by a column vector \underline{o} consisting of uniformly spaced samples of $o(x)$, it being assumed that the object is approximately bandlimited and can therefore be subjected to sampling without appreciable loss of information. In the case of a two dimensional object $o(x, y)$, the vector \underline{o} is constructed by lexicographic ordering^{*} of the samples. For an object consisting of $K \times L$ elements, the vector \underline{o} contains $M = KL$ elements.

The blurring operation to which the object radiance is subjected can be represented by an $M \times M$ matrix $[B]$. Such a matrix can represent a space-invariant or a space-variant blur, depending on the form of its elements. The elements of $[B]$ are samples of the impulse response

^{*}see the Appendix for a detailed definition of this term.

$b(x_1, x_2)$. The classical intensity of the image falling upon the photo-detector is represented by a column vector \underline{i} given by

$$\underline{i} = [B]\underline{o} \quad (11)$$

The detector is assumed to consist of a discrete array of elements, each of which produces a photocount for the observation interval T used. Thus the detected signal is represented by a column vector \underline{d} of length M ; it is assumed that the n^{th} element d_n of \underline{d} is a Poisson random variable, with mean given by

$$\lambda_n = \frac{\eta TA}{h\nu} i_n \quad (12)$$

where A is the area of a detector element, and i_n is the n^{th} element of \underline{i} . Equivalently, we write

$$\underline{\lambda} = \frac{\eta TA}{h\nu} \underline{i} = \frac{\eta TA}{h\nu} [B]\underline{o}, \quad (13)$$

where the n^{th} element of $\underline{\lambda}$ is λ_n .

The detected signal \underline{d} is subjected to linear filtering with the aim of restoration. The restoration filter is represented by a matrix $[H]$, the elements of which are samples of the (possibly space-variant) impulse response $h(x_1, x_2)$. The filter $[H]$ is to be chosen to minimize a certain measure of error between the restored image \underline{r} given by

$$\underline{r} = [H]\underline{d} \quad (14)$$

and an "ideally filtered" object given by

$$\underline{\hat{o}} = [\hat{S}]\underline{o} \quad (15)$$

Here $[\hat{S}]$ is an $M \times M$ matrix of samples of the impulse response $s(x_1, x_2)$ of the ideal filter. The use of a $\hat{\cdot}$ over a matrix, here and

elsewhere in what follows, implies that this matrix has been normalized such that

$$\max_m \sum_n [\hat{S}]_{nm} = 1 \quad (16)$$

where $[\hat{S}]_{nm}$ indicates the $(n,m)^{th}$ element of $[\hat{S}]$.

We define an error column vector $\underline{\epsilon}$ given by

$$\underline{\epsilon} = \underline{\tilde{o}} - \underline{r} = [\hat{S}]\underline{o} - [H]\underline{d} \quad (17)$$

The restoration filter $[H]$ will be chosen to minimize the mean-squared norm of the vector $\underline{\epsilon}$. Equivalently we choose $[H]$ to minimize the quantity

$$\delta = E\{\underline{\epsilon}^t \underline{\epsilon}\} = E\{\text{Tr}(\underline{\epsilon} \underline{\epsilon}^t)\} \quad (18)$$

where t signifies a transpose operation, E is an expectation operator, and $\text{Tr}(\)$ signifies the trace of a matrix (i.e., the sum of the elements along the main diagonal).

(b) Minimizing Mean-Squared-Error

Substituting Eq.(17) in Eq.(18), the mean-squared error to be minimized becomes

$$\begin{aligned} \delta &= E\{\text{Tr}(\underline{\epsilon} \underline{\epsilon}^t)\} \\ &= E\{\text{Tr}(([\hat{S}]\underline{o} - [H]\underline{d})([\hat{S}]\underline{o} - [H]\underline{d})^t)\} \\ &= E\{\text{Tr}([H]\underline{d} \underline{d}^t [H]^t - 2[\hat{S}]\underline{o} \underline{d}^t [H]^t + [\hat{S}]\underline{o} \underline{o}^t [\hat{S}]^t)\} \end{aligned} \quad (19)$$

The expectation can be performed in two steps. First we assume \underline{o} is fixed and take the expectation over only the Poisson statistics

$$E_p(\cdot) = E(\cdot | \underline{o}) \quad (20)$$

Later we take a second expectation over the statistics of \underline{o} . Thus

$$E_p \{ \text{Tr}(\underline{\epsilon} \underline{\epsilon}^t) \} = \text{Tr}([H] E_p \{ \underline{d} \underline{d}^t \} [H]^t - 2[\hat{S}] \underline{o} E_p \{ \underline{d}^t \} [H]^t + [\hat{S}] \underline{o} \underline{o}^t [\hat{S}]^t) \quad (21)$$

Because \underline{d} is Poisson distributed, with statistically independent components (assuming \underline{o} is fixed), it follows that

$$E_p \{ \underline{d} \underline{d}^t \} = \begin{bmatrix} \lambda & 0 \\ 0 & \lambda \end{bmatrix} + \underline{\lambda} \underline{\lambda}^t \quad (22)$$

where the notation is defined by

$$\begin{bmatrix} \lambda & 0 \\ 0 & \lambda \end{bmatrix} = \begin{bmatrix} a_1 & 0 \\ 0 & a_2 \dots a_m \end{bmatrix} \quad (23)$$

It is convenient at this point to normalize the matrices and vectors for future expressions. Again, a matrix $[A]$ is normalized to produce $[\hat{A}]$ by factoring out a constant $C = \max_m \sum_{n=1}^M [A]_{nm}$ from all the columns. A vector \underline{a} is normalized to produce $\underline{\hat{a}}$ by factoring out $\sum_{n=1}^M a_n$ from all elements. As a consequence, $\sum_{n=1}^M \hat{a}_n = 1$. This normalization assumes that the amount of light intercepted by and the net energy loss of the optical system does not change as a point source moves about the object field.

Now, assuming that the energy loss is approximately constant over the field of view, (13) can be written

$$\underline{\lambda} = \frac{1}{k} [\hat{S}] \underline{o} \quad (24)$$

where we have used

$$k \triangleq \frac{h\nu}{b_o \eta TA} \quad (25)$$

$$b_o \triangleq \sum_n [B]_{nm} \quad (\text{assumed identical for all } m).$$

Using (24) in (22), we obtain

$$E_p \left\{ \underline{d} \underline{d}^t \right\} = \frac{1}{k} \begin{bmatrix} \diagdown & 0 \\ [\hat{B}] \underline{o} & \diagup \\ 0 & \end{bmatrix} + \frac{1}{k^2} [\hat{B}] \underline{o} \underline{o}^t [\hat{B}]^t \quad (26)$$

In addition

$$E_p \left\{ \underline{d}^t \right\} = \underline{o}^t [\hat{B}]^t \quad (27)$$

Finally, substitution of (26) and (27) in (21) yields the conditional expectation

$$\begin{aligned} E_p \left\{ \text{Tr}(\underline{\varepsilon} \underline{\varepsilon}^t) \right\} &= \text{Tr} \left([H] \left(\frac{1}{k} \begin{bmatrix} \diagdown & 0 \\ [\hat{B}] \underline{o} & \diagup \\ 0 & \end{bmatrix} + \frac{1}{k^2} [\hat{B}] \underline{o} \underline{o}^t [\hat{B}]^t \right) [H]^t \right. \\ &\quad \left. - \frac{2}{k} [\hat{S}] \underline{o} \underline{o}^t [\hat{B}]^t [H]^t + [\hat{S}] \underline{o} \underline{o}^t [\hat{S}]^t \right). \end{aligned} \quad (28)$$

The remaining task in calculating the desired error measure is to average over the object ensemble. Applying such an average to Eq. (28) yields

$$\begin{aligned} \bar{\epsilon} &= \text{Tr} \left([H] \left(\bar{N} \begin{bmatrix} \diagdown & 0 \\ [\hat{B}] \underline{o} & \diagup \\ 0 & \end{bmatrix} + \bar{N}^2 [\hat{B}] [\hat{\mathcal{X}}_o] [\hat{B}]^t \right) [H]^t \right. \\ &\quad \left. - 2k \bar{N} [\hat{S}] [\hat{\mathcal{X}}_o] [\hat{B}]^t [H]^t + k^2 \bar{N}^2 [\hat{S}] [\hat{\mathcal{X}}_o] [\hat{S}]^t \right) \end{aligned} \quad (29)$$

where the expected number of photoevents, \bar{N} , in the image is

$$\bar{N} = E_0 \left\{ \frac{1}{k} \sum_n \bar{c}_n \right\} \quad (30)$$

In addition, the definitions

$$\begin{aligned} \hat{\underline{c}} &\triangleq E_0 \{ \underline{c} \} / \sum_n \bar{c}_n \\ [\check{\mathbf{X}}_0] &\triangleq \frac{E \{ \underline{c} \underline{c}^t \}}{k^2 \bar{N}^2} \end{aligned} \quad (31)$$

have been used. This is not a totally unusual normalization for $[\mathbf{X}_0]$

since

$$E_0 \left\{ \left[\sum_n ([\hat{\mathbf{B}}] \underline{c})_n \right]^2 \right\} = k^2 \left(\bar{N}^2 + \sigma_\lambda^2 \right) \quad (32)$$

where

$$\sigma_\lambda^2 = \text{variance of } \left(\sum_n \lambda_n \right) \quad (33)$$

Thus, if the variance of the number of photoevents per image is small, and the covariance of λ is reasonably constant over the field of view, then

$$[\check{\mathbf{X}}_0] = [\hat{\mathbf{X}}_0] \quad (34)$$

The final problem is to find the filter matrix $[\mathbf{H}]$ that minimizes the error measure \mathcal{E} of Eq.(29). Fortunately, the answer to this problem is available in the literature and can be directly employed here (Ref.1). The filter matrix that minimizes \mathcal{E} is given by

$$[\mathbf{H}] = k \bar{N} [\hat{\mathbf{S}}] [\check{\mathbf{X}}_0] [\hat{\mathbf{B}}]^t \left(\begin{bmatrix} \hat{\mathbf{S}} & 0 \\ 0 & [\hat{\mathbf{B}}] [\check{\mathbf{X}}_0] [\hat{\mathbf{B}}]^t \end{bmatrix} + \bar{N} [\hat{\mathbf{B}}] [\check{\mathbf{X}}_0] [\hat{\mathbf{B}}]^t \right)^{-1}. \quad (35)$$

It should be emphasized that this filter will in general be space variant, depending on the properties of $[\hat{\mathbf{S}}]$, $[\hat{\mathbf{B}}]$, $\hat{\underline{c}}$, and $[\check{\mathbf{X}}_0]$.

(c) Minimum Mean-Squared Error

In order to specify the performance of the optimum filter, it is helpful to have an expression for the minimum mean-squared error ϵ_{\min} actually achieved. If we substitute expression (35) for the optimum filter in expression (25) for the mean-squared error, we obtain

$$\epsilon_{\min} = k^2 \bar{N}^2 \text{Tr} \left([\hat{S}] [\hat{X}_0] \left([I] - [\hat{B}]^t \begin{bmatrix} [\hat{B}] \hat{\underline{0}} & 0 \\ 0 & [\hat{B}] \hat{\underline{0}} \end{bmatrix} + \bar{N} [\hat{B}] [\hat{X}_0] [\hat{B}]^t \right)^{-1} [\hat{B}] [\hat{X}_0] [\hat{S}]^t \right) \quad (36)$$

where $[I]$ is the identity matrix. Sometimes it is useful to have the minimum mean-squared-error in the alternative form

$$\epsilon_{\min} = k^2 \bar{N}^2 \text{Tr} \left([\hat{S}] [\hat{X}_0] [\hat{S}]^t - [H] [\hat{B}] [\hat{X}_0] [\hat{S}]^t \right) \quad (37)$$

For purposes of comparison with the continuous case, it is interesting to manipulate (36) further, yielding the form

$$\epsilon_{\min} = k^2 \bar{N}^2 \text{Tr} \left([\hat{S}] [\hat{X}_0] \left(\begin{bmatrix} [\hat{B}] \hat{\underline{0}} & 0 \\ 0 & [\hat{B}] \hat{\underline{0}} \end{bmatrix} + \bar{N} [\hat{B}] [\hat{X}_0] [\hat{B}]^t \right)^{-1} \begin{bmatrix} [\hat{B}] \hat{\underline{0}} & 0 \\ 0 & [\hat{B}] \hat{\underline{0}} \end{bmatrix} [\hat{S}]^t \right) \quad (38)$$

Note the similarity of this result to expression for minimum mean-squared error in the continuous case (derived in our earlier reports),

$$\epsilon_{\min} = k^2 \bar{N}^2 \iint_{-\infty}^{\infty} \frac{|\hat{S}|^2 \hat{\underline{0}}^2 d\Omega_X d\Omega_Y}{1 + \bar{N} |\hat{B}|^2 \hat{\underline{0}}^2} \quad (39)$$

(see, for example, Eq.(7) of RADC-TR-77-165). An important difference is, of course, that Eq.(38) holds in the space-variant case, while Eq.(39) is valid only for a space-invariant filter.

(d) Image Quality Measures

Two different image quality measures were found useful in the continuous case. One, which we called the "image quality factor", Q , was defined as the ratio of the "signal" energy at the output of the restoration filter to the mean-squared error ("noise") at the output. A second, which we called the "restored bandwidth", $\Delta\tilde{\Omega}$, was equivalent bandwidth of the cascade of the blur and deblurring filters.

Concentrating first on the quality factor Q , we note that in the discrete case, the expected energy in the detected signal is given by the inner product

$$\begin{aligned} E\{\underline{d}^t \underline{d}\} &= E\{\text{Tr}(\underline{d} \underline{d}^t)\} \\ &= \text{Tr}\left(\frac{1}{N} \begin{bmatrix} & & 0 \\ & [\hat{\theta}] \hat{\theta} & \\ 0 & & \end{bmatrix} + \frac{1}{N^2} [\hat{\theta}] [\hat{\chi}_0] [\hat{\theta}]^t\right) \end{aligned} \quad (40)$$

The "signal" portion of this energy is given by the second term,

$$\frac{1}{N^2} \text{Tr}([\hat{\theta}] [\hat{\chi}_0] [\hat{\theta}]^t) \quad (41)$$

After passage through the restoration filter $[H]$, the signal energy at the output is given by

$$\Delta \hat{\Delta} \frac{1}{N^2} \text{Tr}([H] [\hat{\theta}] [\hat{\chi}_0] [\hat{\theta}]^t [H]^t) \quad (42)$$

Substitution of the optimum $[H]$ yields

$$d = k^2 \bar{N}^2 \text{Tr} \left([\hat{S}] [\hat{\mathcal{X}}_0] [\hat{B}]^t \left(\begin{bmatrix} \hat{B} \hat{\mathcal{X}}_0 \\ 0 \end{bmatrix} + \bar{N} [\hat{B}] [\hat{\mathcal{X}}_0] [\hat{B}]^t \right)^{-1} \right. \\ \left. \cdot [\hat{B}] [\hat{\mathcal{X}}_0] [\hat{B}]^t \left(\begin{bmatrix} \hat{B} \hat{\mathcal{X}}_0 \\ 0 \end{bmatrix} + \bar{N} [\hat{B}] [\hat{\mathcal{X}}_0] [\hat{B}]^t \right)^{-1} [\hat{B}] [\hat{\mathcal{X}}_0] [\hat{S}]^t \right) \quad (43)$$

The image quality factor Q is then defined as

$$Q \triangleq \frac{d}{\delta_{\min}} \quad (44)$$

As for the second measure of image quality, restored bandwidth, the situation is a bit more difficult, since for a space-variant system there is no unique bandwidth that can be specified. Stated another way, there is in general a different bandwidth associated with every point in the filtered image.

In the continuous analysis of a space-invariant system, the restored bandwidth $\Delta\tilde{\omega}$ was defined by

$$\pi (\Delta\tilde{\omega})^2 = \iint_{-\infty}^{\infty} |\hat{B}\hat{H}| d\omega_x d\omega_y \quad (45)$$

If the product of \hat{B} and \hat{H} (the normalized transfer functions of the blur and deblur filters, respectively) is non-negative and real, as is generally the case in practice, then Eq. (45) can be rewritten

$$\pi (\Delta\tilde{\omega})^2 = \iint_{-\infty}^{\infty} \hat{h}(-\xi, -\eta) \hat{b}(\xi, \eta) d\xi d\eta \quad (46)$$

where \hat{b} and \hat{h} are the inverse Fourier transforms of \hat{B} and \hat{H} , respectively. This expression is the integral of the product of the two impulse responses, centered at the origin in this case. The same

restored bandwidth would be obtained by integrating the product of the impulse responses centered at any point in output plane, a consequence of the fact that both the blur and the restoration filter are space invariant.

In the space-variant case, the product of \hat{b} and \hat{h} will yield functions with different areas, depending on where this product is centered in the output plane (x,y) . The integral becomes

$$\pi(\Delta\tilde{\Omega}(x,y))^2 = \iint_{-\infty}^{\infty} \hat{h}(x,y;\xi,\eta) \hat{b}(\xi,\eta;x,y) d\xi d\eta \quad (47)$$

and is clearly a function of which output coordinates (x,y) are chosen.

The discrete analogy to Eq. (47) would be to define the restored bandwidth at the n^{th} output point by

$$\pi(\Delta\tilde{\Omega}_n)^2 = ([\hat{H}][\hat{B}])_{nn} \quad (48)$$

where for matrix $[A]$, the symbol $([A])_{nn}$ is the n^{th} diagonal element of $[A]$. Since this quantity depends on the point n , it is not of itself a useful measure of image quality. However, all three of the following definitions would be useful:

$$\pi(\Delta\tilde{\Omega}_{AV})^2 = \frac{1}{M} \text{Tr}([\hat{H}][\hat{B}]) \quad (49a)$$

$$\pi(\Delta\tilde{\Omega}_{MAX})^2 = \text{Maximum diagonal element of } [\hat{H}][\hat{B}] \quad (49b)$$

$$\pi(\Delta\tilde{\Omega}_{MIN})^2 = \text{Minimum diagonal element of } [\hat{H}][\hat{B}]. \quad (49c)$$

These definitions may be regarded as yielding average, maximum and minimum restored bandwidths, respectively.

(e) The Stationary, Shift-Invariant Case

We now consider the form taken by the various results above in the special case of a shift-invariant matrix $[H]$. In this case, $\frac{1}{M}$ is a

constant vector with elements $\frac{1}{M}$, while the matrix $[\check{\mathbf{x}}_0]$ takes on toeplitz form. In addition, the ideal filter matrix $[\hat{\mathbf{S}}]$ and the blur matrix $[\hat{\mathbf{B}}]$ take toeplitz^{*} form, and the matrix $\begin{bmatrix} & & 0 \\ & [\hat{\mathbf{B}}] \hat{\mathbf{0}} & \\ 0 & & \end{bmatrix}$ will be of the form $\frac{1}{M} [\mathbf{I}]$.

If the covariance function of the object and the point-spread functions of the ideal and blur filters are sufficiently narrow, the toeplitz matrices above can be replaced by circulant^{*} approximations. With this substitution the post-compensation filter matrix becomes

$$[\mathbf{H}_c] = k \bar{N} [\hat{\mathbf{S}}_c] [\check{\mathbf{x}}_{0_c}] [\hat{\mathbf{B}}_c]^t \left(\frac{1}{M} [\mathbf{I}] + \bar{N} [\hat{\mathbf{B}}_c] [\check{\mathbf{x}}_{0_c}] [\hat{\mathbf{B}}_c]^t \right)^{-1} \quad (50)$$

where the subscript c indicates a circulant approximation.

The quality factor Q becomes in this case

$$Q = \frac{\text{Tr}([\mathbf{H}_c] [\hat{\mathbf{B}}_c] [\check{\mathbf{x}}_{0_c}] [\hat{\mathbf{B}}_c]^t [\mathbf{H}_c]^t)}{k^2 \text{Tr}([\hat{\mathbf{S}}_c] [\check{\mathbf{x}}_{0_c}] \left(\frac{1}{M} [\mathbf{I}] + \bar{N} [\hat{\mathbf{B}}_c] [\check{\mathbf{x}}_{0_c}] [\hat{\mathbf{B}}_c]^t \right)^{-1} \frac{1}{M} [\mathbf{I}] [\hat{\mathbf{S}}_c]^t)} \quad (51)$$

The equivalent bandwidth becomes

$$\pi (\Delta \Omega_{AV})^2 = \frac{1}{M} \text{Tr}([\hat{\mathbf{H}}_c] [\hat{\mathbf{B}}_c]) \quad (52)$$

For any circulant matrix $[\mathbf{C}]$, the identity

$$[\mathbf{C}] = [\mathbf{F}] [\Lambda_c] [\mathbf{F}]^{-1} \quad (53)$$

holds, where $[\mathbf{F}]$ is the two-dimensional discrete Fourier transform (DFT) matrix, and $[\Lambda_c]$ is a diagonal matrix with elements that are the eigenvalues of $[\mathbf{C}]$. Using this fact, the $[\mathbf{H}]$ matrix and the quality measures can be rewritten in the forms

$$[\mathbf{H}_c] = k \bar{N} [\mathbf{F}] [\Lambda_S] [\Lambda_{\check{\mathbf{x}}_0}] [\Lambda_B]^* \left([\mathbf{I}] + \bar{N} [\Lambda_B] [\Lambda_{\check{\mathbf{x}}_0}] [\Lambda_B]^* \right)^{-1} [\mathbf{F}]^{-1} \quad (54)$$

^{*}See the Appendix for a detailed definition of this term.

$$Q = \frac{\text{Tr} \left([\mathcal{F}] [\Lambda_H] [\Lambda_B] [\Lambda_{\mathcal{X}_0}] [\Lambda_B]^* \left([I] + \bar{N} [\Lambda_B] [\Lambda_{\mathcal{X}_0}] [\Lambda_B]^* \right)^{-1} [\mathcal{F}]^{-1} \right)}{k^2 \left(\text{Tr} \left([\mathcal{F}] [\Lambda_S] [\Lambda_{\mathcal{X}_0}] \left([I] + \bar{N} [\Lambda_B] [\Lambda_{\mathcal{X}_0}] [\Lambda_B]^* \right)^{-1} [\Lambda_S]^* [\mathcal{F}]^{-1} \right) \right)} \quad (55)$$

$$\pi(\Delta\Omega_{AV})^2 = \frac{1}{M} \text{Tr} \left([\mathcal{F}] [\Lambda_H] [\Lambda_B] [\mathcal{F}]^{-1} \right) \quad (56)$$

Note that the eigenvalues of a circulant matrix are the values of the DFT of the first column of the circulant matrix.

Because of the diagonal forms of (54), (55) and (56), it is convenient to represent the n^{th} component of the DFT of the restored image by $R(n)$, and the n^{th} component of the DFT of the detected image by $D(n)$. Then we have

$$R(n) = \frac{k \bar{N} \hat{S}(n) \hat{B}^*(n) \hat{\phi}_0(n)}{1 + \bar{N} |\hat{B}(n)|^2 \hat{\phi}_0(n)} D(n) \quad (57)$$

and

$$Q = \frac{\bar{N}^2 \sum_n \frac{|\hat{B}(n)|^4 |\hat{S}(n)|^2 \hat{\phi}_0^3(n)}{\left(1 + \bar{N} |\hat{B}(n)|^2 \hat{\phi}_0(n) \right)^2}}{\sum_n \frac{|\hat{S}(n)|^2 \hat{\phi}_0(n)}{1 + \bar{N} |\hat{B}(n)|^2 \hat{\phi}_0(n)}} \quad (58)$$

where $\hat{\phi}_0$ is the DFT of $\check{\mathcal{X}}_0$. Further,

$$\pi(\Delta\Omega_{AV})^2 = \frac{1}{M} \sum_n \hat{H}(n) \hat{B}(n) \quad (59)$$

These last three equations are exact analogs of the results presented in earlier reports for the continuous case, the only difference being the replacement of integrals by discrete sums. Thus the results of the more general space-variant analysis do indeed reduce to the results obtained in earlier analyses of the space-invariant case.

V. NUMERICAL COMPUTATIONS IN PROGRESS

At this time computations are being performed on four simple initial cases. These initial cases all involve one dimensional objects only, and each has at most one shift-variant or non-stationary factor. One case is totally stationary and shift-invariant.

For each of these cases the image quality factor Q of (44) and the three forms of the restored bandwidth (49) are being computed. In the three non-stationary or shift-variant cases the image quality measures are being computed using a series of shift-invariant restoration filters $[H]$. In the totally stationary, shift-invariant case only the optimum shift-invariant $[H]$ are being used. For the three non-stationary or shift-variant cases the image quality measures are also being computed using the optimum shift-variant filter of (35). The shift-variant and shift-invariant filter performances will then be compared.

Of our initial cases, case 1 is totally stationary and shift-invariant. For this case $\hat{\underline{o}}$ is assumed to be

$$\hat{\underline{o}} = \frac{1}{M} \underline{1} \quad (60)$$

where $\underline{1}$ is a vector of all ones. In general the following relation holds

$$[\underline{x}_0] = [\underline{\phi}_0] + \underline{\bar{o}} \underline{\bar{o}}^t \quad (61)$$

where

$$[\underline{\phi}_0] = E((\underline{o} - \underline{\bar{o}})(\underline{o} - \underline{\bar{o}})^t) \quad (62)$$

In the stationary case the covariance matrix $[\underline{\phi}_0]$ is assumed to be

$$[\underline{\phi}_0] = \sigma^2 [I] \quad (63)$$

For this shift-invariant case the blur is assumed to produce a Gaussian point-spread function. In each of the following three cases, only

one of the above assumptions about $\hat{\underline{o}}$, $[\phi_o]$, and $[b]$ will be changed. Thus it should be possible to determine what factors are most improved by the shift-variant filter $[h]$.

In case II the blur $[b]$ is no longer assumed to be shift-invariant, but instead is assumed to have a position dependent width which increases near the edges of the image. All other factors are assumed the same as case I.

In case III the object ensemble is assumed to have a Gaussian mean intensity profile centered in the field of view. All other factors are again assumed the same as case I.

In the last case, case IV, the auto-covariance function $[\phi_o]$ is assumed to be of the form

$$([\phi_o])_{ij} = \sigma^2 \delta_{ij} \exp \left\{ - \left(\frac{i - \frac{M}{2}}{w} \right)^2 \right\} \quad (64)$$

where

$$\delta_{ij} = \begin{cases} 1 & i = j \\ 0 & i \neq j \end{cases}$$

$$w = \text{a width parameter} \quad (65)$$

$$\sigma^2 = \text{center variance}$$

Thus it is assumed that the object ensemble has a non-stationary variance which decreases toward the edges of the object. As in the above two cases, the other factors are assumed the same as case I.

Results of these calculations will be presented in our next technical report.

REFERENCES

1. H.C. Andrews and B.R. Hunt, Digital Image Restoration, Prentice-Hall, N.J. 1977.

APPENDIX

In this appendix we define several specialized terms used in the body of the report.

Lexicographic ordering

It is common practice in the image processing community to represent two-dimensional arrays of samples by vectors. If, for example, an image is sampled on a two-dimensional sampling grid, it is perhaps most naturally represented by a matrix of sample values:

$$[I] = \begin{bmatrix} i_{11} & i_{12} & \cdots & i_{1N} \\ i_{21} & i_{22} & \cdots & i_{2N} \\ \vdots & & & \\ i_{N1} & i_{N2} & \cdots & i_{NN} \end{bmatrix} \quad (A.1)$$

For mathematical purposes, it is often convenient to reduce this matrix to a vector \underline{i} . This is accomplished by scanning the matrix row by row to create a one-dimensional array of samples:

$$\underline{i} = \begin{bmatrix} i_{11} \\ \vdots \\ i_{1N} \\ i_{21} \\ \vdots \\ i_{2N} \\ \vdots \\ i_{NN} \end{bmatrix} \quad (A.2)$$

The vector \underline{i} is said to have been constructed by lexicographic ordering of the matrix $[I]$.

Toeplitz Matrix

A matrix $[A]$ is said to be a Toeplitz matrix if it has the property that, whenever $j - k = m - n$, the elements $[A]_{jk}$ and $[A]_{mn}$ are equal. An example of a Toeplitz matrix is given below:

$$[A] = \begin{bmatrix} 2 & 4 & 7 & 5 \\ 9 & 2 & 4 & 7 \\ 6 & 9 & 2 & 4 \\ 8 & 6 & 9 & 2 \end{bmatrix} \quad (A.3)$$

The covariance matrix of a wide-sense stationary random process is always a Toeplitz matrix.

Circulant Matrix

A matrix $[C]$ is called circulant if each of its rows is a right cyclic shift of the previous row by one element. The first row must be a right cyclic shift of the last row by one element. An example of a circulant matrix is given by

$$[C] = \begin{bmatrix} 2 & 4 & 7 & 5 \\ 5 & 2 & 4 & 7 \\ 7 & 5 & 2 & 4 \\ 4 & 7 & 5 & 2 \end{bmatrix} \quad (A.4)$$

Note that by "cyclic shift" we mean the shifting of rows must be of the "wrap-around" type. That is, when an element is shifted out on the right, it immediately reappears on the left. Note, also that all circulant matrices are Toeplitz in form.

It is common practice in image processing to approximate some forms of Toeplitz matrices by constructing circulant matrices from them. If a Toeplitz matrix has only a few localized non-zero diagonals, a circulant

approximation is often constructed by replacing some of the zero diagonals with non-zero diagonals thus forming the result into the circulant form.

As an example, the Toeplitz matrix

$$[T] = \begin{bmatrix} 7 & 5 & 1 & 0 & 0 & 0 & 0 \\ 3 & 7 & 5 & 1 & 0 & 0 & 0 \\ 2 & 3 & 7 & 5 & 1 & 0 & 0 \\ 0 & 2 & 3 & 7 & 5 & 1 & 0 \\ 0 & 0 & 2 & 3 & 7 & 5 & 1 \\ 0 & 0 & 0 & 2 & 3 & 7 & 5 \\ 0 & 0 & 0 & 0 & 2 & 3 & 7 \end{bmatrix} \quad (A.5)$$

can be converted to the circulant matrix

$$[T^c] = \begin{bmatrix} 7 & 5 & 1 & 0 & 0 & 2 & 3 \\ 3 & 7 & 5 & 1 & 0 & 0 & 2 \\ 2 & 3 & 7 & 5 & 1 & 0 & 0 \\ 0 & 2 & 3 & 7 & 5 & 1 & 0 \\ 0 & 0 & 2 & 3 & 7 & 5 & 1 \\ 1 & 0 & 0 & 2 & 3 & 7 & 5 \\ 5 & 1 & 0 & 0 & 2 & 3 & 7 \end{bmatrix} \quad (A.6)$$

by changing the three upper right and lower left zero elements.

Computations using circulant matrices can be performed faster than those for Toeplitz matrices because the discrete Fourier transform can be utilized. As the fraction of diagonals of the Toeplitz matrix which are non-zero decreases, the circulant approximation approaches the original matrix, and the errors associated with the use of the circulant approximation can be shown to decrease.

*MISSION
of
Rome Air Development Center*

RADC plans and conducts research, exploratory and advanced development programs in command, control, and communications (C³) activities, and in the C³ areas of information sciences and intelligence. The principal technical mission areas are communications, electromagnetic guidance and control, surveillance of ground and aerospace objects, intelligence data collection and handling, information system technology, ionospheric propagation, solid state sciences, microwave physics and electronic reliability, maintainability and compatibility.

